*Journal of* ELECTRICAL ENGINEERING, VOL 73(2022), NO6, 396–404

sciendo
PAPERS

# Lightweight ultra-wideband antenna array equipped with thin frequency selective surface for high-gain applications

**Pratyancha Prasad, Shiva Nand Singh, Akhilesh Kumar**[1]

This article begins with an explanation of a frequency selective surface, also known as an FSS, which is used to increase gain across a wide frequency range. The proposed unit design is a modified combination of circular and square elements with two cross dipoles and a T-type structure at the inner side. In the second step of the process, a single wideband antenna that covers the same range as FSS is designed and then analyzed in terms of its gain and radiation patterns. After that, an antenna array was built using the same solo structure in order to take advantage of the benefits that come with using an array system. The array is made up of elements that are CPW fed. A ground-backed T-shaped power divider network with additional shorting pins is used to supply power to the entire array. In the fourth step, an array of the FSS unit cell has been positioned beneath the UWB solo antenna and its array in order to investigate the possibility of improved gain and radiation pattern. The FSS equivalent lumped circuit model is presented here for validation purposes. It has been determined that the results of the experiment and the simulation are consistent with one another. In contrast to the structures that have been reported in the past, the newly developed model possesses a greater bandwidth, a higher gain, and a lower profile.

K e y w o r d s: ultra-wideband antenna array, X-band, Ku-band

## 1 Introduction

The recent development of frequency selective surfaces, also known as FSSs, has piqued the interest of researchers due to the numerous applications that can be accomplished with these surfaces. These applications include spatial filtering, radar cross section (RCS) reduction, absorbers, and polarizers [1,2]. Recent research has focused on structures that are based on metamaterials (MTMs) and meta surfaces (MSs), specifically in this context. This is because these new classes of materials help to control the undesirable losses in the wave propagation direction by exclusively controlling the electromagnetic (EM) properties. The reason for this is that these new classes of materials have recently emerged. Metallic patches of varying sizes and shapes are arranged in regular patterns to form FSSs.

One of the goals is to boost the antenna's performance in addition to the FSS's filtering abilities. There is still a lot of work being done to figure out how to get greater performance by cleverly leveraging the metal shapes. A variety of FSS structures [3] and their applications in performance enhancement of antennas have already been investigated [4-9]. Beginning with multi-layered wideband polarization-insensitive FSS, their corresponding circuit models were investigated so that wide band performance could be analyzed. Next, single and multi-layer configurations of very angularly stable FSS BP and BS filters were developed. Then, a proposed active FSS uses p-i-n diodes, which have no effect on absorption performance over the target band. On the other hand, the design of ultra-wideband (UWB) monopole antennas for use in a wide variety of wireless applications is a subject of antenna research that is both active and promising. Monopole antennas typically have a relatively high back lobe radiation, which contributes to their generally poor peak gain. As a result, FSS has been hailed as a significant achievement for its ability to enhance the gain and directionality of UWB antenna systems.

Since the FCC's announcement that the $3.1-10.6$ GHz band would be open to unlicensed usage, research into UWB antennas has exploded [10]. These antennas often feature omnidirectional radiation patterns and modest gains (typically between 0 and 5 dBi).

Use of unidirectional UWB antennas allows users to sidestep the performance hit that comes with omni directionality. Furthermore, a communication system with increased speed and decreased power consumption is possible due to the directivity. As a result, it is preferable to create a UWB antenna with high-directivity and characteristics of unidirectional radiation.

This is one of the reasons why antenna arrays are gaining popularity. By structuring the antenna array in such a way that it consists of multiple smaller antennas that are isolated from one another, it is possible to cover the same bandwidth range with a more directional and high gain. These properties are required in great majority of applications, some of which include radio astronomy, communications, radars, satellites, and electronic warfare and electronic warfare.

[1] Department of Electronics and Communication Engineering, National Institute of Technology, Jamshedpur, India, pratyancha.p17@gmail.com

https://doi.org/10.2478/jee-2022-0054, Print (till 2015) ISSN 1335-3632, On-line ISSN 1339-309X

In this study, we use the fundamental concept of increasing the gain by putting a frequency selective surface layer below the antenna. This layer acts like a reflector, and its purpose is to redirect the radiation that is emitted by the antenna in the opposite direction. The gain of the antenna improves whenever the waves radiated by the antenna and the waves reflected by FSS are in phase with one another. Therefore, first we present two-dimensional FSS, which has a fractional bandwidth (FBW) of 147.7% and has a single metallization layer. The bandwidth of −10 dB extends from 3.01 GHz all the way up to 20 GHz. The configuration of the unit cell that has been suggested features a modified combination of circular and square elements, as well as two cross dipoles and a T-type structure on the inner side. After that, a stand-alone UWB antenna with the same range coverage as the FSS is designed and afterwards analyzed. Thereafter, an antenna array was made utilizing the same single construction in order to take advantage of the benefits that are associated with employing an array system. These benefits include increased signal strength and less interference. The array is constructed out of elements that receive their feeding from CPW. For the purpose of supplying power to the complete array, a ground-backed T-shaped power divider network with additional shorting pins has been utilized. The remainder of the parts of the paper are organized as shown below: The construction and explanation of the FSS unit cell, solo antenna, and its array are covered. The constructed prototype, the operation of the antenna and its array with FSS, as well as its measurement results, are discussed in detail.

## 2 Design

### *2.1 Proposed frequency selective surface*

*Unit Cell Design:*

The suggested unit cell has a design that includes one metallic layer that is printed on a single side of the FR-4 substrate. This layer has a thickness of 0.8 mm ($0.008\lambda_0$), a relative permittivity of 4.4, and a loss tangent of 0.02. The overall FSS is laid out so that the $x, y$, and $z$ axes, in that order, correspond to the length, breadth, and height, respectively. In order to determine the final characteristics of the proposed FSS, the HFSS software is utilised.

The top view and the side view of the cell is shown in Fig. 1. The major objective of the proposed FSS is to achieve consistent wide bandwidth (BW) while maintaining insensitive polarization. Figure 2(a) depicted the simulations results of the FSS operating as a broad band reflector for TE polarization, the normal angle of incidence and linearity characterizes the phase of reflection coefficient. According to the transmission characteristics, when compared to the reference level of −10 dB, band stop or reflector response ranging from 3.01 to 20 GHz has been proposed for the FSS. The structure's behavior in terms of absorption is poor. Figure 2(b) shows the absorptivity of the structure with FSS which is less the 1% in the majority of the operating band. In addition to having low absorptivity, the features of reflection lend support to the band- stop proposed for use in the FSS as a reflector. Figure 2(c) shows the polarization insensitivity of the structure. As the orientation of E-field varies from 0-90°, the transmission characteristics show a stable response.

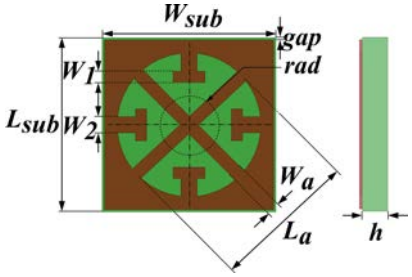


**Fig. 1.** Unit cell: Top and side view

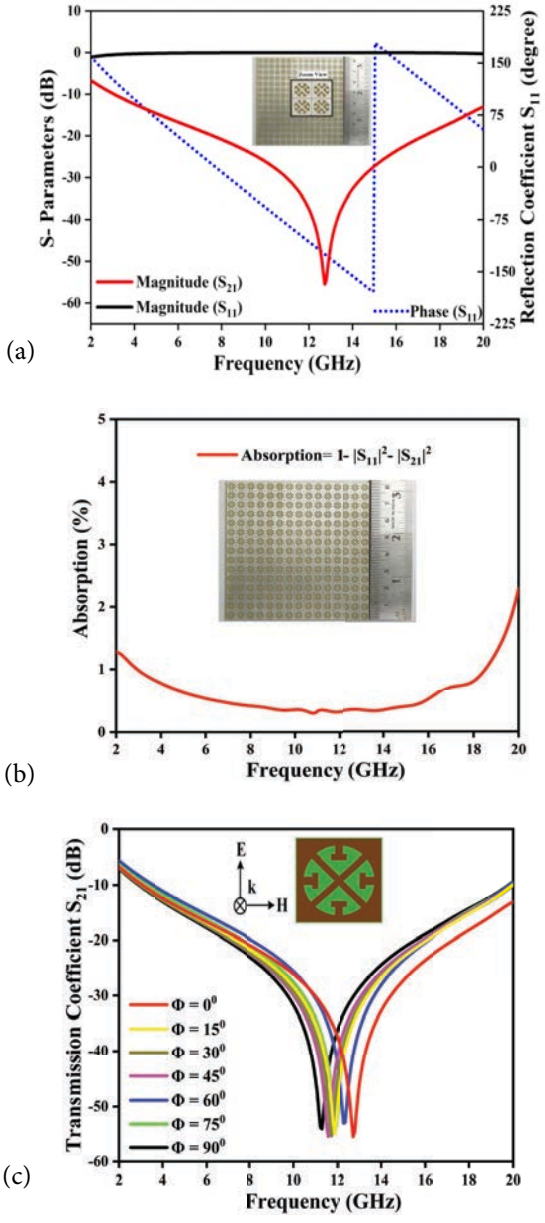


**Fig. 2.** Plot of: (a) – magnitude and phase of reflection and transmission coefficients, (b) – absorptivity of the FSS, and (c) – magnitude of transmission coefficient for various angles of polarization

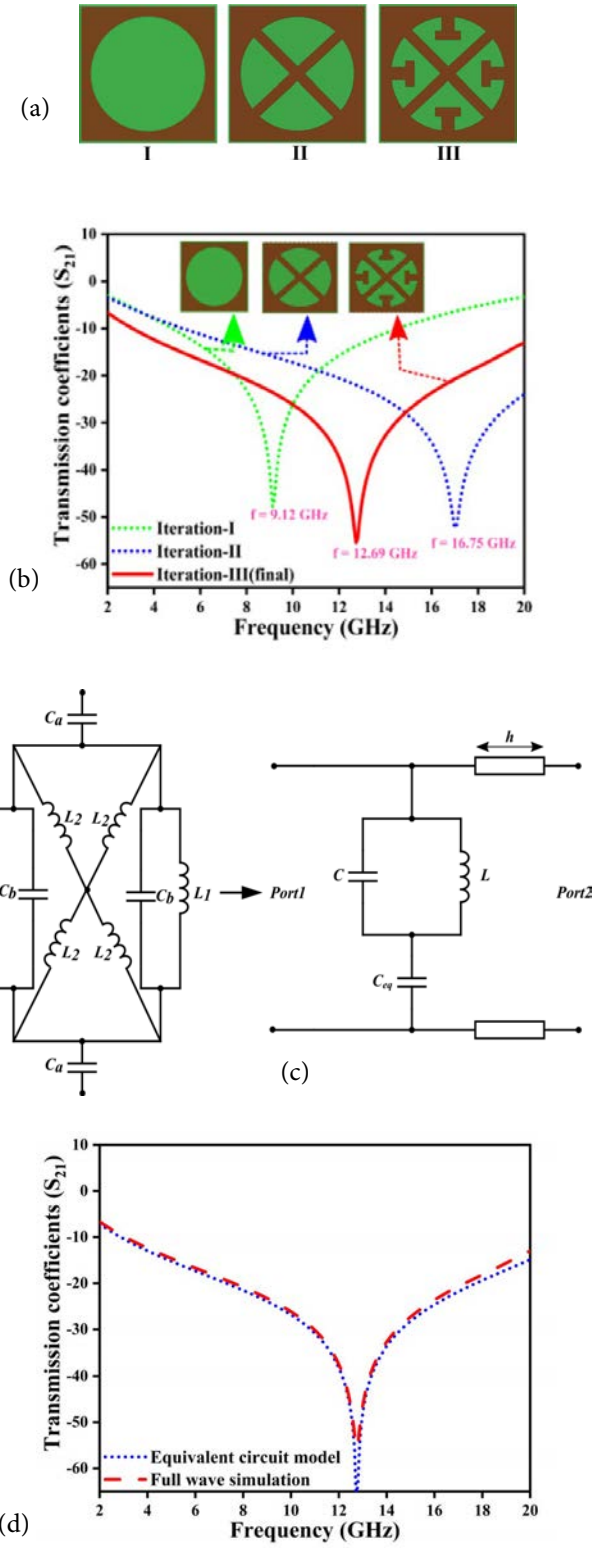


**Fig. 3.** Unit cell (a) – iterations, (b) – plot of transmission coefficients ($S_{21}$), (c) – equivalent circuit model, and (d) – plot of transmission coefficient ($S_{21}$) of circuit model and full wave simulation

Following is a list of the optimised parameters (dimensions in mm): $W_{\text{sub}} = L_{\text{sub}} = 5.45$, gap $= 0.05$, rad $= 2.26$, $W_1 = 0.35$, $W_2 = 0.5$, $W_a = 0.35$, $L_a = 4.5$ and $h = 0.8$.

*Unit Cell Iterations:*

The iterations that are included in the process of designing FSS unit cells are depicted in Fig. 3(a). When the metallization is added, it is done so in order to fine-tune the inductances and capacitances so that a wide band-stop response can be achieved. In Fig. 3(b), the transmission coefficients of the various iterations is depicted. The structure of Iteration (i) which is a simple circular slot inside a square patch with a radius of $r$, has a resonance frequency of 9.12 GHz, and a broadband response that ranges from 4.79 to 14.54 GHz. Additionally, the bandwidth of Iteration I structure is 9.75 GHz.

Iteration II is absolutely necessary in order to achieve wideband frequencies higher than 20 GHz. By connecting two cross dipoles with a thickness of 0.35 mm in an orthogonal position with the inner circumference of the circular slot, the path of the flowing current, which is actually greatest towards the edge, is increased. Because the new bandwidth ranges from 5.25 GHz all the way up to more than 20 GHz, the resonance frequency has moved to 16.75 GHz.

Iteration III includes the addition of a T-type structure in the free space of the inner circumference of the circular slots that are positioned between two cross dipoles. This leads to an increase in the entire band, which now extends from 3.01 to around 20 GHz in frequency range. The primary goal of this addition is to reduce the frequency from 5.45 GHz to a level that is below the lower range of UWB, which is 3.01 GHz, while also maintaining the wideband spanning up to 20 GHz.

*Circuit Analysis:*

The equivalent circuit is shown in Fig. 3(c). Considering a single ring, it can be broken down as follows. The outer metallic ring will have an inductance $L_1$. The inner cross metallic arms parallel to the wave impinging on the surface will present an inductance $L_2$ due to its inherent width. There is a small gap between the metallic arm and the outer edge of the substrate. Thus, a capacitance will develop between two neighbouring metallic arms of the unit cell ($C_a$). Further the gap between the arms of adjacent rings will also generate capacitance ($C_b$). This capacitance, in series with the adjacent unit cell capacitance ($C_a$) can be equivalently modelled as $C$ for the outermost ring. The $L$ and $C$ of ring 1 in parallel generate a tank circuit. This is in series with the additional capacitance $C_{eq}$ which accounts for stay capacitances in the ring. The structure is repeated for each ring taking into account the respective capacitances and inductances to generate the correct waveform of the full wave simulation. Fig. 3(d) shows the result of the equivalent circuit model and the full wave simulation.

### 2.2 Proposed wideband single antenna

*Antenna Design*

Figure 4 depicts the final configuration of the single monopole antenna. This pattern makes use of a combinational patch that is both elliptical and circular, and

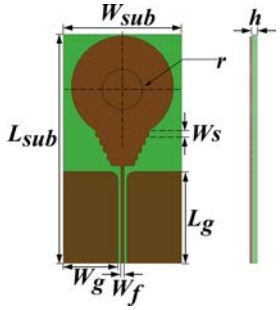


**Fig. 4.** Geometry of the proposed antenna: top view and side view

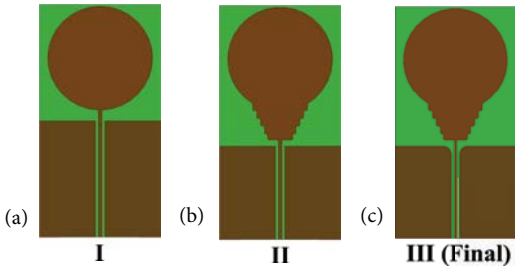


**Fig. 5.** Unit cell (a) – iteration I, (b) – iteration II, and (c) – iteration III (final)

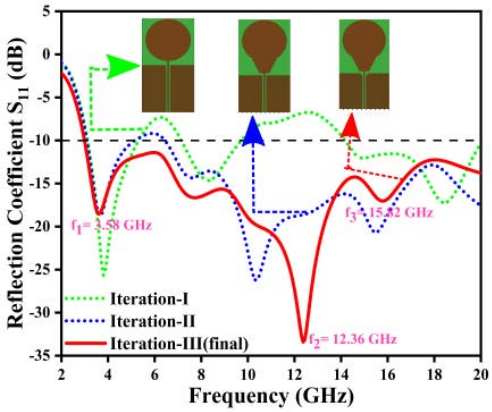


**Fig. 6.** $S_{11}$ of various iterations of proposed antenna

it features fine stepped transitions between suitable dimensions. A CPW feed is going to be used to excite the proposed antenna. A substrate made of FR-4 epoxy that is 0.8 mm thick and has a permittivity of 4.4 is used to design a resonator that has an overall dimension of $0.15\lambda_0 \times 0.30\lambda_0$, where, $\lambda_0$ denotes the wavelength that is connected with the frequency that is lower in this particular case. This is done to ensure that the antenna is able to function correctly and emit signals across the full wideband. The following is a list of the various measurements that can be taken for the antenna. These measurements are as follows: $L_{\text{sub}} = 30$, $W_{\text{sub}} = 15.5$, $W_{\text{f}} = 0.4$, $L_{\text{g}} = 12$, $W_{\text{g}} = 7.15$, $W_{\text{s}} = 0.8$, $r = 6.7$, $h = 0.8$. All units are in mm.

The process of obtaining a wideband impedance matching is one of the most difficult tasks involved in the wideband antenna. It is dependent on a number of factors including the substrate's thickness, the dielectric properties of the substrate, and the topology of the ground plane and feed line. According to the studies that have been done and published, there is the potential for transitions between an elliptical or circular central conductor and a CPW feed to be designed in such a way as to improve the return loss and bandwidth of a UWB antenna. This causes the real part of the impedance to be high, while at the same time the reactance is reduced to a minimum, providing an impedance match across a broad frequency spectrum. The stepped transitions are effective in reducing the return loss, increasing the bandwidth, and providing controlled resonances [11].

A more in-depth illustration of the stages of evolution indicated for the proposed single monopole antenna is provided in Fig. 5, which can be seen here. During the process of designing the antenna, there are two iterations that take place in order to arrive at the final dimensions that are optimal for the design.

A straightforward circular patch was chosen for the radiator in Iteration I, Fig. 5(a). This patch was fed with a CPW-feed, which provides a superior wideband response when compared to full-ground. In this iteration, there are three bands with resonant frequencies located at 3.80 GHz, 8.33 GHz, and 18.56 GHz. The first band ranges from 3.12 to 5.28 GHz, the second from 7.20 to 9.85 GHz, and the third from 14.11 to up to 20 GHz. The FBW for these band are 51.4%, 31.4%, and 34.6% respectively.

During the iteration II, Fig. 5(b), a stepped impedance match is introduced between the feedline and the patch. This leads to a better impedance response at the higher frequency, which results in the combination of two bands into a single band with a resonance frequency of 10.20 GHz and a frequency bandwidth of 104.3%. Also, a minor improvement was made in the lower frequency range, specifically between 3.04 GHz and 5 GHz, with the resonant frequency located at 3.6 GHz.

In the final iteration, *ie* III, represented by Fig. 5(c), the CPW grounds were filleted, which resulted in a significant improvement in the impedance match across the entire band of the spectrum. We have obtained a complete band with a frequency range from 3.01 GHz to 20 GHz, with resonant frequencies located at 3.58 GHz, 12.36 GHz, and 15.82 GHz. The reflection coefficients of each iteration is shown in Fig. 6.

### *2.3 Proposed wideband antenna array*

To achieve the same level of performance as a single large antenna, it is possible to use an array consisting of several smaller antennas that are isolated from one another. Because of their high directivity and high gain, antenna arrays are becoming increasingly popular. These characteristics are necessary for the vast majority of applications, including radio astronomy, communications, radars, satellites, electronic warfare, and electronic warfare. In order to generate a good directional pattern, the fields of the antenna arrays need to interfere with one another in a way that is constructive in the desired direction and destructive in all other directions that are not desired.

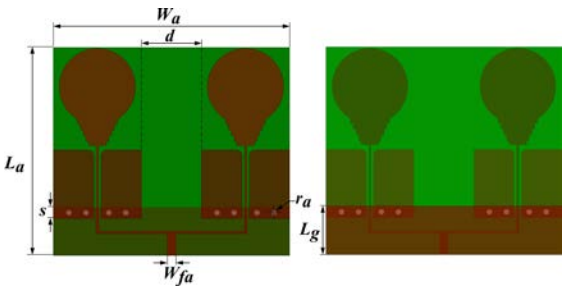


**Fig. 7.** Antenna array with dimensions: top view and rear view

Recent years have seen a proliferation of research proposals pertaining to UWB antenna array. One of the most well- known types of existing UWB antennas is the tapered slot antenna array, also known as the Vivaldi antenna array [12]. These arrays are well-liked because of their scan capabilities, high gain, and wide band. These array antennas have a large impedance bandwidth, however while scanning they emit undesired radiation and loss polarization purity. From what has been discussed above, it can be deduced that Vivaldi arrays are a good fit for high gain systems, but that their maintenance needs are significant [13].

Another one is the spiral antenna, these has the best combination of bandwidth, circular polarizations, and size for wideband applications among all frequency-independent antennas. Typically, spiral antennas have a wide frequency response. However, they can't be used as phased arrays owing of their bulky design and lackluster gain. However, later on, UWB phased arrays make advantage of the spiral arrays [14,15]. The spiral array antenna's bandwidth is limited by size, which grows with working frequency. But, increasing bandwidth causes greater element spacing, lowering the lowest operational frequency. This creates grating lobes at smaller scan angles.

The sinuous antenna is another element that provides low gain, operates in the UWB range, and has a frequency- independent nature. Because of its characteristics, it is an excellent choice for use in UWB applications such as radars, electronic warfare, and high-sensitivity requirements [16]. But it suffers from the drawbacks of having a restricted bandwidth over scanning and losing its polarizations [17].

On the other hand, the design of the microstrip planar antenna array is characterized by popular in wireless communication devices due to its advantageous characteristics, which include a low profile, the ability to conform to mounting hosts, a small size, and the capacity to support linear and circular polarization [18].

This array presented in this paper has two radiators that are shaped and oriented in the same manner as the radiator of the single prototype antenna. This array is designed to improve the array's performance in comparison to the single prototype antenna.

A novel concept in this design is the use of a second conductive layer on the bottom side of the array, with four vias of equal diameter (0.1 mm) connecting it to the top layer. The excitation network, represented by the stripline power divider (T-junction) in each array design, makes sure that each radiator is excited at the same rate shown in Fig. 7. The following is a list of the various measurements that can be taken for the array of antennas.: $L_a = 36.5,\ W_a = 41.5,\ L_g = 8.5,\ W_{fa} = 1.5,\ r_a = 0.1,\ \mathrm{d} = 10.5,\ s = 2$ and $h = 0.8$. All units are in mm.

## 3 Results and discussion

The proposed antenna, its array, and the FSS reflector all have been successfully fabricated and measured. There were four separate attempts made to carry out the measuring procedure. The discussion will begin with an examination of the proposed solo antenna and its array, followed by an examination of the solo antenna with FSS, and finally a discussion of the antenna array with FSS. In either case, five distinct parameters – the reflection coefficient ($S_{11}$), the gain (dB),the efficiency, the radiation patterns, and the performance comparison – are assessed and analyzed.

The vector network analyzer (N5222A) by Agilent Technologies, which has an operating range of 10 MHz to 26.5 GHz is used to measure the antennas ($S_{11}$) coefficients. It is of the utmost importance that the distance separating the wide band model that has been proposed (both solo and in array form) and the FSS be an integer multiple of the wavelength at the central frequency. However, because FSS operates across a wide frequency range,

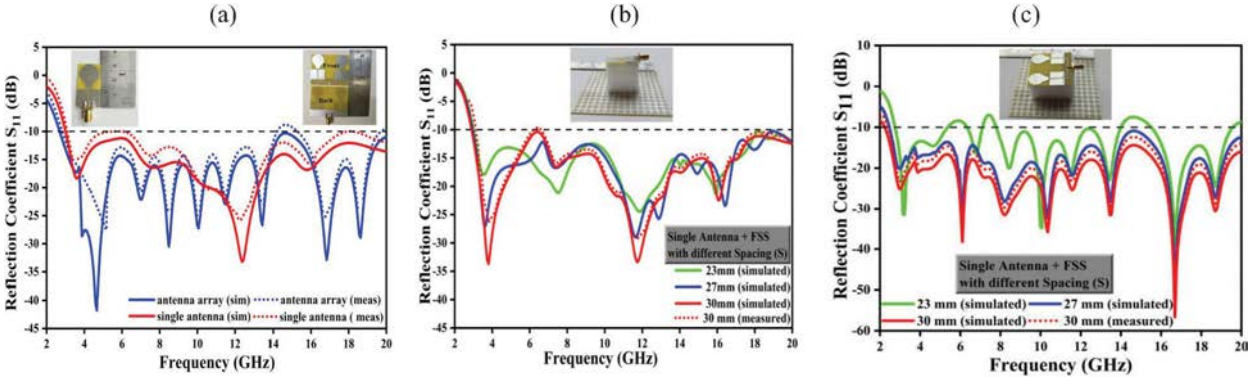


**Fig. 8.** Simulated and measured $S_{11}$ of (a) – antenna and its array, (b) – antenna with FSS, and (c) – antenna array with FSS

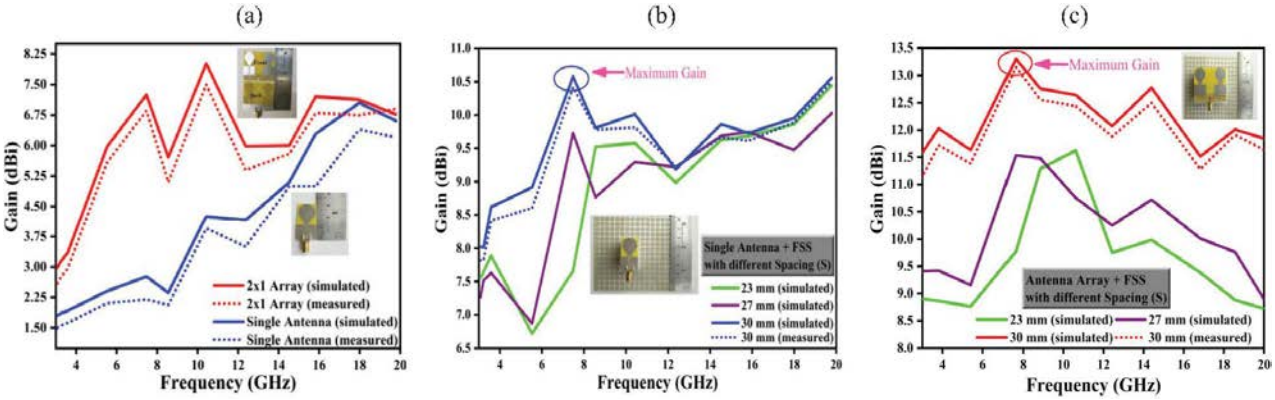


**Fig. 9.** Simulated and measured gain of the (a) – antenna and its array, (b) – antenna with FSS, and (c) – antenna array with FSS

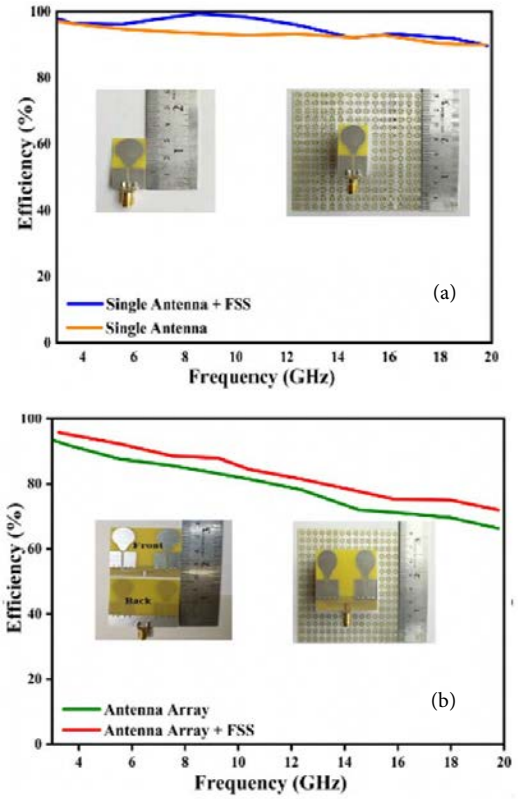


**Fig. 10.** Simulated efficiency of (a) – single element; with and without FSS, and (b) – antenna array with and without FSSS

the distance between the FSS layer and the antenna must be carefully considered in order to achieve the same complete wideband and highest possible gain. The proposed antenna and its array are both assembled on the topside of an elements FSS that has been compiled by replicating the unit cell.

The parametric study is conducted on three distinct spaces, namely 23 mm, 27 mm, and 30 mm respectively. Carefully utilizing styrofoam with a thickness of 30 mm, the gap between the antenna and FSS can be realized. Foam is utilized because it has almost no impact on the antenna's functionality.

### *3.1 Reflection coefficient*

The comparison of the measured and simulated reflection coefficient ($S_{11}$) of the proposed antenna and antenna array is shown in Fig. 8(a). The findings of the simulation of the single antenna with no FSS indicate that it has a $-10$ dB impedance bandwidth of 16.99 GHz. This bandwidth spans the range of 3.01 -20 GHz, and the measured value is slightly off due to differences in fabrication error and measurement devices.

In case of antenna array $-10$ dB is same as the single antenna almost but with multiple resonances. Reason is in order to achieve maximum directivity, $\lambda/2$ is the ideal distance between individual antenna elements. Since $\lambda/2$ only represents a single frequency, this poses a problem for wideband antennas. Regarding our situation, we have maintained the antenna at a distance of 10.5 mm. However, for lower frequencies, this separation becomes less than $\lambda/2$, and for higher frequencies, it becomes greater than $\lambda/2$. Resonances can be attributed to this type of coupling.

A comparison of the solo antenna and its array after it has been integrated with FSS is shown in Fig. 8(b),(c) for each of the three different heights (23 mm, 27 mm, and 30 mm). The FSS is positioned below the antenna in such a way that it is able to reflect the radiation that is coming from the antenna in the opposite direction. The gain of the antenna is increased when the waves reflected by the FSS are in phase with the radiation produced by the antenna. Therefore, a gap must be present between the UWB antenna and the proposed FSS in order to ensure the constructive interference of reflected waves with directly radiated waves from the antenna. A rough estimate of the distance that separates the antenna and the FSS is, [19,20]

$$\varphi - 2\beta H = 2n\pi, \quad n = \cdots -1, 0, 1, \ldots \tag{1}$$

### *3.2 Gain and efficiency*

The simulated and measured gains of a single antenna and an antenna array are depicted in Fig. 9(a). A single antenna has a maximum gain of 7.01 dBi, which can be attained to its full potential. It is noticeable that across the entirety of the frequency range, gain steadily increases as one advances from lower to higher frequency ranges. In the case of an array, the range expands substantially to approximately 1.5 dBi. An antenna array is capable of

**Table 1.** Analysis of the proposed work with literature present in analogous applications

| Ref | FSS unit cel ($mm^3$) | Antenna ($mm^3$) | Gain (dB) solo/FSS | Improvement Layer | Type | Frequency bands[1)] $S_{11}$ | $S_{21}$ | Bandwidth (%) FSS | Antenna |
|---|---|---|---|---|---|---|---|---|---|
| [4] | $10.4\times9.8\times3.2$ | $45\times45\times1.6$ | 1.8/5.76 | 1 | meta | 2.4-2.7 | 2.2-3 | 11 | 33 |
| [5] | $13.5\times13.5\times0.64$ | $72\times72\times0.51$ | 6.3/7.9 | 1 | FSS | 3.1-11 | 3-8 | 112 | 91 |
| [6] | $10.8\times10.8\times0.4$ | $35\times30\times0.8$ | 5.4/8.5 | 2 | FSS | 3.1-10 | 3.2-13.5 | 105 | 123 |
| [7] | $7\times7\times0.8$ | $70\times70\times1.6$ | 4.6/9 | 3 | FSS | 5.2-8.3[2)] | 5-8.5 | 46 | 52 |
| [8] | $8.25\times8.25\times0.64$ | $50\times50\times1.52$ | 6.5/8.5 | 1 | FSS | 3-11 | 3-12 | 114 | 120 |
| [9] | $5\times5\times1.6$ | $50\times50\times1.6$ | 7/11 | 1 | FSS | 2.2-12.7 | 2.1-12.6 | 140 | 143 |

[1)] FSS and antenna, in GHz, [2)] 10 dB bandwidth

| | Size ($mm^3$) | Gain (dB) | Improvement | Frequency bands[1)] | Efficiency |
|---|---|---|---|---|---|
| This work | $5.45\times5.45\times0.8$ (Cell)<br>$15\times30\times0.8$ (Antenna) | 7.01 (single)<br>8.20 (array)<br>10.6 (single, FSS)<br>13.4 (array, FSS) | Single layer FSS | $S_{11}$, $S_{21}$<br>3.01–20 GHz | FSS,Array<br>147.8 % |

achieving a gain of up to 8.20 dBi at its highest feasible setting. In this case the gain is more than that of a single antenna and is also almost constant at the higher frequency range, which is something that stands out across the board in terms of frequency range.

Figure 9(b),(c) demonstrates that the results at 30 mm are substantially more satisfying when the antenna is loaded with FSS (b), as well as when the array is loaded with FSS (c). When compared to a standalone antenna (a), the total range of gain is approximately 6.5 dBi higher. This is an improvement. The maximum gain that can be achieved with this arrangement is somewhere in the neighbourhood of 10.6 dBi, despite the fact that the gain is higher than 8 dBi across the whole range. Finally, the workflow is considered to have been finished after the FSS has been loaded into the antenna array. Although the gain is greater than 11.5 dBi throughout the whole range, the highest gain that can be reached with this arrangement is somewhere in the neighbourhood of 13.4 dBi.

The antenna efficiency for single element with and without FSS is shown in Fig. 10(a). The addition of FSS causes a slight increase in efficiency at lower frequencies. However, for array, the increase in efficiency is increased significantly with the addition of FSS, Fig. 10(b).

### *3.3 Radiation pattern*

Normalized power distributions in the E-and H-planes for the proposed antenna with FSS layers at 3.08, 7.42, and 15.84 GHz, as measured and simulated, are shown in Fig. 11. The antenna's omnidirectional H-plane pattern and correct broadside E-plane directive pattern imply it can be used for a wide range of frequencies. As the measured and simulated outcomes are consistent, we can conclude that sufficient matching has been accomplished. The majority of the variations seen in the pattern plot can be attributed to errors in production, reflection from the environment, and cable losses during measurement.

### *3.4 Performance comparison*

The potential of the proposed FSS loaded antenna and its array is shown by a comparison of its performance to that of existing, state-of-the-art works in the field (Tab. 1). The dimensions of the UWB antenna and the FSS :

$15\,\text{mm}\times30\,\text{mm}\times0.8\,\text{mm}$,

$5.45\,\text{mm}\times5.45\,\text{mm}\times0.8\,\text{mm}$,

are smaller than those of the antennas shown in [4-8], with the exception of the antennas shown in [9]. While carefully observing [9], despite the fact that the size of the unit cell is slightly smaller than intended, the monitoring UWB antenna is significantly larger than the size. Additionally, the BW coverage range is somewhat limited. As a result, the suggested FSS loaded antenna array is a promising option for highgain UWB applications due to its small size, high gain, and increased bandwidth.

## 4 Conclusions

In this paper lightweight and thin FSS is proposed and its use to increase gain across a wide frequency range is analyzed. An FSS is used to enhance the gain. The design of the unit cell is quite condensed and elongated at the same time. The bandwidth range has been improved from 3.01 GHz to 20 GHz sufficiently to act as effective reflector in the entire UWB range, in addition to the X (8-12 GHz) and Ku (12-18 GHz) bands. After that, a single, thin, and compact wideband antenna that covers the same range as FSS is designed, and its gain, efficiency and radiation patterns are studied afterwards. The greatest possible gain from this is 7.01 dBi (single antenna). An antenna array was built using the same solo structure in order to take advantage of the benefits that are associated with employing an array system. The array is constructed out of elements that receive their feeding from CPW. A ground-backed T-shaped power divider network that includes additional shorting pins has been utilized

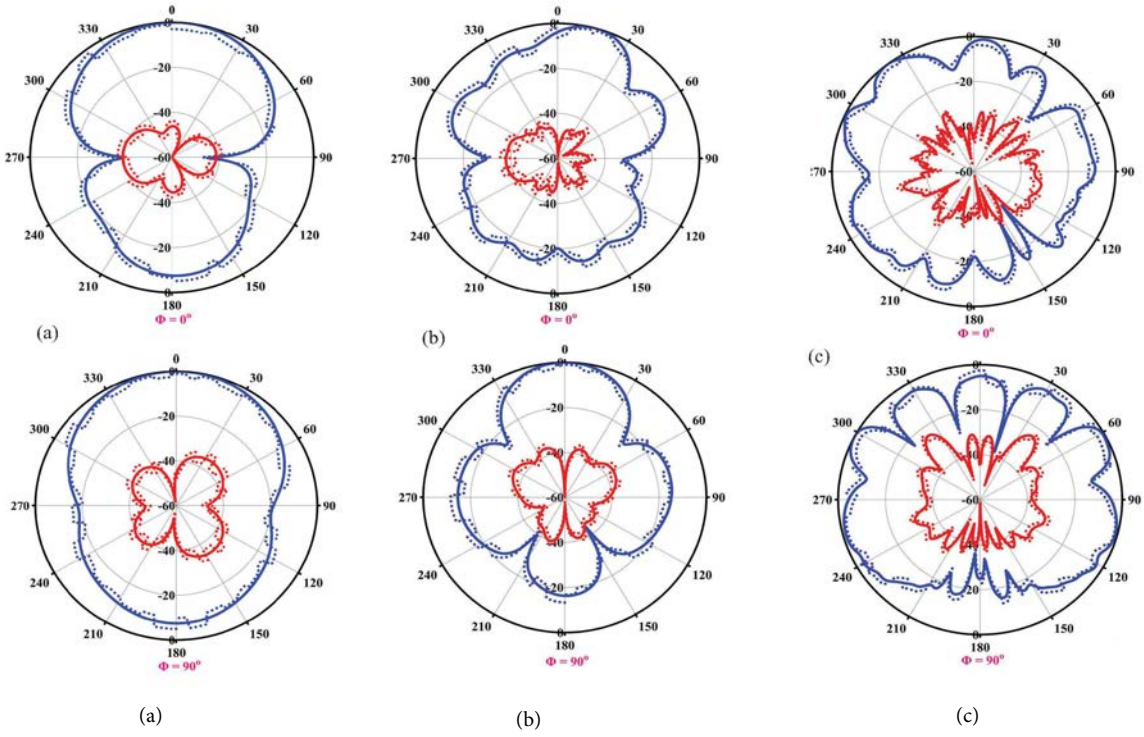


**Fig. 11.** Simulated and measured co- and cross-polarization radiation pattern of antenna array with FSS at (a) – 3.08 GHz, (b) – 7.47 GHz, and (c) – 15.84 GHz

to feed the array. Finally, an array of the FSS unit cell measuring 81.75 mm × 81.75 mm has been placed directly beneath the UWB solo antenna and its array in order to investigate the possibility of improved gain and radiation pattern. The gain in case of array is 8.2 dBi. In this particular instance, the gain has been considerably increased to 10.6 dBi (antenna with FSS) and 13.4 dBi (array with FSS) and has become almost stable across the entirety of the range. It has been determined that the outcomes of the experiment and the simulation are comparable to one another and support this hypothesis.

## References


[1] B. A. Munk, *Frequency Selective Surfaces*, New York: John Wiley & Sons, Ltd, 2000.

[2] F. Costa, A. Monorchio, and G. Manara, "Efficient analysis of frequency- selective surfaces by a simple equivalent-circuit model", *IEEE Antennas and Propagation Magazine*, vol. 54, no. 4, pp. 35-48, 2012.

[3] A. Chatterjee and S. K. Parui, "A triple-layer dual-bandpass frequency selective surface of third order response with equivalent circuit analysis", *International Journal of RF and Microwave Computer-Aided Engineering*, vol. 30, no. 2, p. e22047, 2020.

[4] M. Ameen and R. K. Chaudhary, "Metamaterial-based wideband circularly polarised antenna with rotated V-shaped metasurface for small satellite applications", *ELECTRONICS LETTERS*, vol. 55, no. 7, pp. 365-366, APR 4 2019.

[5] R. Yahya, A. Nakamura, M. Itami, and T. A. Denidni, "A novel UWB FSS-based polarization diversity antenna", *IEEE Antennas and Wireless Propagation Letters*, vol. 16, pp. 2525-2528, 2017.

[6] S. Kundu, A. Chatterjee, S. Jana, and S. Parui, "A compact umbrella- shaped UWB antenna with gain augmentation using frequency selective surface", *Radioengineering*, vol. 27, no. 2, pp. 448-454, 06 2018.

[7] A. Chatterjee and S. Parui, "Gain enhancement of a wide slot antenna using a second-order bandpass frequency selective surface", *Radioengineering*, vol. 24, no. 2, pp. 455-461, 06 2015.

[8] Y. Yuan, X. Xi, and Y. Zhao, "Compact UWB FSS reflector for antenna gain enhancement", *IET Microwaves*, Antennas & Propagation, vol. 13, no. 10, pp. 1749-1755, 2019.

[9] A. Al-Gburi, I. B. M. Ibrahim, Z. Zakaria, B. H. Ahmad, A. B. S. Shairi, and M. Y. Zeain, "High gain of UWB planar antenna utilising FSS reflector for UWB applications", *Computers*, Materials & Continua, vol. 70, no. 1, pp. 1419-1436, 01 2022.

[10] F. Commission *et al*, "First report and order in the matter of revision of part 15 of the commission's rules regarding ultra-wideband transmission systems", *Docket 98-153 FCC 02*, vol. 48, 2002.

[11] P. Prasad, S. N. Singh, and A. Kumar, "A compact high-gain key- shaped monopole antenna for RF sensitive environment, and X-Ku-band applications", *Frequenz*, vol. 76, no. 5-6, pp. 297 -307, 2022.

[12] J. Prouza and Z. Raida, "Practical design of Ku band vivaldi antenna array", *Journal of Electrical Engineering*, vol. 71, no. 5, pp. 347-352, 2020.

[13] J. T. Logan, R. W. Kindt, and M. N. Vouvakis, "Low cross-polarization vivaldi arrays", *IEEE Transactions on Antennas and Propagation*, vol. 66, no. 4, pp. 1827-1837, 2018.

[14] I. Hinostroza, R. Guinvarc'h, and R. L. Haupt, "The design of wide band planar arrays of spiral antennas", *2011 IEEE International Symposium on Antennas and Propagation* (APSURSI), pp. 609-611, 2011.

[15] R. Guinvarc'h, "Dual polarization wideband interleaved spiral antenna array", *IET Conference Proceedings*, pp. 94-94(1), January 2007.

[16] Y. Kang, K. Kim, and W. R. Scott, "Modification of sinuous antenna arms for UWB radar applications", *IEEE Transactions on Antennas and Propagation*, vol. 63, no. 11, pp. 5229-5234, 2015.

[17] N. Steenkamp, D. I. L. d. Villiers, and N. Mutonkole, "Wideband pyramidal sinuous antenna for reflector antenna applications", *2017 11th European Conference on Antennas and Propagation* (EUCAP), pp. 2291-2295, 2011.

[18] M. Garbaruk, "A planar four-element UWB antenna array with stripline feeding network", *Electronics*, vol. 11, no. 3, 2022.

[19] N. Hussain, M.-J. Jeong, J. Park, and N. Kim, "A broadband circularly polarized fabry-perot resonant antenna using a single-layered PRS for 5G MIMO applications", *IEEE Access*, vol. 7, pp. 42 897-42 907, 2019.

[20] N. Hussain, M.-J. Jeong, A. Abbas, T.-J. Kim, and N. Kim, "A metasurface-based low-profile wideband circularly polarized patch antenna for 5G millimeter-wave systems", *IEEE Access*, vol. 8, pp. 22 127- 22 135, 2020.

Received 14 September 2022

**Pratyancha Prasad**, Research scholar, NIT Jamshedpur, was born in Damoh, Madhya Pradesh India in 1984. She received her Bachelor's degree in Electronics and Communication from SGSITS, Indore in 2006 and Masters in Electronics and Communication Engineering from College of Engineering, Pune in 2009. From 2010 till 2019, she worked as an Assistant Professor in BACET, Jamshedpur. Her research interests include ultra-wideband antennas (UWB), Frequency Selective Surfaces and Metasurfaces.

**Shiva Nand Singh**, Professor, NIT Jamshedpur, was born in Jamshedpur, Jharkhand India in 1957. He received his Bachelor's degree in Electronics and Communication Engineering from BIT Mesra, Ranchi, Jharkhand, India in 1979. Master's degree in Electrical Engineering (EE) from Ranchi University, Jharkhand, India, in 1991. He received PhD degree from the Department of EE, (NIT), Jamshedpur, Jharkhand, India in 2009. He has published more than 80 papers in National and International Journals. He is a member of the Editorial Board of International journals and chaired sessions in International Conferences. He is also Co-ordinator of Govt. of India sponsored VLSI SMDP-C2SD Project at NIT Jamshedpur, Jharkhand, India. His current research interest includes Machine learning, Solar Technology, VLSI, Industrial Electronics, and Drives.

**Akhilesh Kumar**, Associate Professor, NIT Jamshedpur, was born in Patna, Bihar India in 1964. He received his BSc Engg degree from Bhagalpur University, Bhagalpur, India in 1987. MSc Engg degree from Bihar Institute of Technology, Sindri, India in 1994 and the PhD degree from Magadh University, Bodhgaya, India in 2016. He has more than 25 publications. His research interests include wideband antennas, Frequency Selective Surfaces, Deep Learning, Image Processing, and Digital VLSI.